A FAST BEAM INTERLOCK SYSTEM FOR THE ADVANCED PHOTON SOURCE PARTICLE ACCUMULATOR RING*

J. Dooling[†], M. Borland, K. Harkay, R. Keane, B. Micklich, C. Y. Yao, ANL, Argonne, IL 60439, USA

Abstract

The feasibility of a fast beam interlock system for the Advanced Photon Source (APS) Particle Accumulator Ring (PAR) is considered for high-charge operations. This system would be based on detection of Cerenkov light generated from lost electrons passing through high-purity, fused-silica fiber optic cable. The cable acts as both radiator and light pipe to the photomultiplier tube (PMT). Results from a prototype installation have shown excellent sensitivity, linearity, and reproducibility after 10,000 hours of operation, with little change in transmission. The high sensitivity allows a more accurate measure of low-level loss than do current monitors and faster response than installed gamma or neutron detectors. These features will be important as we modify the PAR to accept higher energy electrons from the linac. Initial calibration measurements of the prototype system against radiation monitors for various loss scenarios are discussed. Comparison of the scenarios with simulations are presented.

INTRODUCTION

High-purity, fused silica fiber optic (FO) cables have been demonstated as sensitive, Cherenkov-radiation-based beam loss monitors (BLMs) at a number of light sources [1–3]. At the Advanced Photon Source (APS), FO cables have been used to set timing and amplitude for the abort kicker used to prevent quenching in superconducting undulators (SCUs) [4]. The FO detectors were also able to roughly quantify the lost charge threshold for quenching the SCUs. More recently, FO detectors have been explored beam loss characterization on the APS PAR [5]. During present APS operations, the PAR typically stores 1-2 nC of charge from the linac at 375-425 MeV for subsequent injection into the booster synchrotron; however, for the planned APS upgrade (APS-U) [6], 20 nC of charge must be accumulated using 10-20 linac pulses.

MCNP SIMULATIONS

MCNP v6.2 [7] was used to calculate radiation dose both inside and outside the PAR bulk concrete shielding. Figure 1 shows a plan view of the MCNP model, including 1.3-m-thick ordinary concrete shielding, beam vacuum chamber, and dipole magnets. Areas that are normally occupied are located south, southeast, and east of the PAR enclosure. The circumference of the PAR is 30.667 m, and the beam
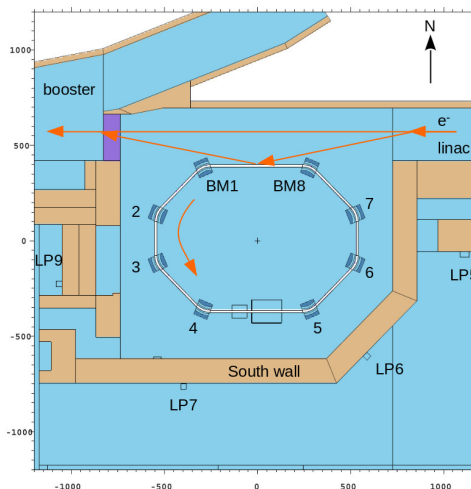

Figure 1: MCNP PAR model; dimensions are given in cm.

direction is counterclockwise as indicated by the arrow. Figure 1 also shows the locations of paired neutron and gamma detectors outside the shield wall. These units, designated with the prefix LP, are used to shut off the linac beam if excessive radiation limits are seen (10 mrem/h gamma, 3 mrem/h neutron) [8].

PAR beam studies have been carried out for a number of loss scenarios; in these scenarios [9], beam is lost each octant of the ring. In loss scenario 3, beam is lost in the west end of the ring and heads toward the south wall after interacting with the beam pipe and bending magnet. We wish to know the dose received both inside and outside the shield wall; in the former case to evaluate the dose received by the fiber and in the latter to determine personnel protection requirements. The simulation evaluates the loss of 2 nC at an energy of 500 MeV (1 J). Presently, 500 MeV is the maximum energy envisioned for PAR APS-U operations. Simulated radiation levels outside the shield wall inform us about the speed with which the interlock must operate. Figure 22 shows the distribution of effective dose on both sides of the south shield wall for Scenario 3. The maximum dose outside the shield wall is ~0.1 mrem, implying a dose rate of 3 mrem/s if beam is lost in this manner at the maximum 30 Hz rate. 10 CFR 835 [10] requires the effective dose received by non-radiation workers be less than 100 mrem/y; therefore, a response at 30 Hz is not necessary and a 0.5- or 1.0-second integration period is acceptable for the interlock.

Inside the shielding, the fiber receives about 6.1 mrem of electrons/positrons and 28.7 mrem of photons (not shown) for a total of roughly 35 mrem/pulse (assuming radiation weighting factors of one for electrons and photons). Darkening of high-purity fused silica has been observed at dose
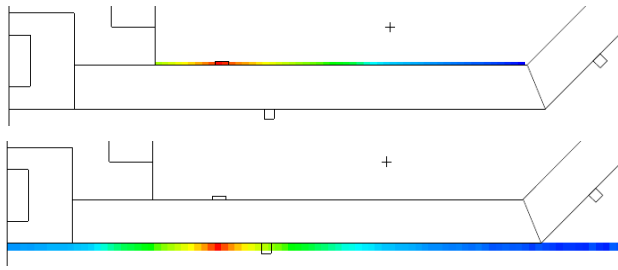
Figure 2: MCNP dose predictions along the PAR south shield wall for 2 nC, 500 MeV beam loss. Top: inside e^+/e^- dose, peak: 6.1 mrem; bottom: outside photon dose; peak: 0.095 mrem. See Fig. 1 for geometry reference.

levels of 1 MGy (100 Mrad) [11]; for continuous beam loss at 30 Hz, this dose would be delivered in about 3 years of operation.

MEASUREMENTS

Two 4-m-length FO cables were deployed for radiation detection in the PAR tunnel. Both consist of 61, 200-μm diameter, 220-μm clad, fused-silica fibers in a close-pack array yielding a diameter of 2-mm and numerical aperture of 0.22. One cable was installed on the beam vacuum chamber, the other on the inside of the shield wall at beam elevation; Figure 3 illustrates both locations. The fiber, which serves as both radiator and light guide, is terminated at one end by a reflector, while the other end is coupled to a photomultiplier tube (PMT) that resides within lead shielding.
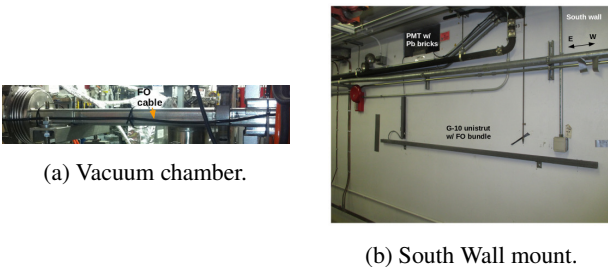
(a) Vacuum chamber.

(b) South Wall mount.

Figure 3: Prototype FO detectors mounted on the PAR vacuum chamber and south wall.

Transmission and Heartbeat

Radiation-induced darkening in BLM FO cables, which reduces transmission and thus sensitivity to beam loss, has been studied previously [11, 12]. To test transmission, an amber LED was driven with a 100-ns, fixed-amplitude pulse as the PMT HV bias was varied over its useful range (-400 to -900 V); see Fig. 4. Peak LED emission wavelength was observed at 589 nm (FWHM of 15 nm), a spectral range where transmission degradation from radiation is most likely [11]. Results of transmission measurements for both prototype FO bundles recorded over several years are presented in Figure 5. These data show that the transmission has not
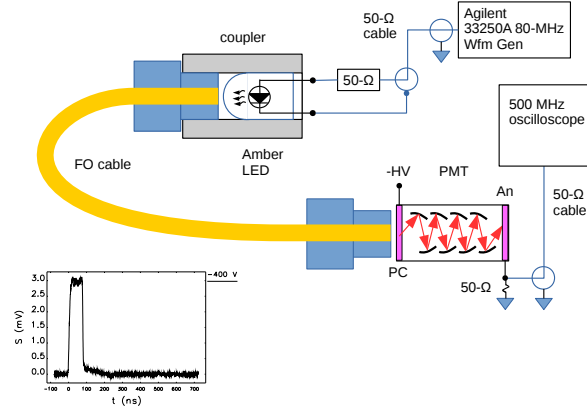

Figure 4: FO transmission test schematic. Inset shows the PMT output test pulse at a bias of -400 V.
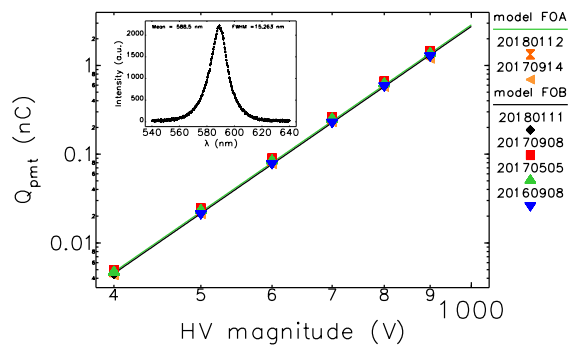

Figure 5: Prototype FO cable transmission with HV bias over the last two years of running. Inset shows the LED spectrum used for these measurements.

changed over the last two years of irradiation and observation nor should it based on the loss actually seen by the fibers. The fit to PMT data shows that the device is healthy and working as expected. Fig. 5 also plots the expected response of the PMT with HV bias, according the relation,

$$Q_{pmt} = Q_{ref} \left(\frac{V}{V_{ref}} \right)^{n-1}, \qquad (1)$$

where Q_{ref} is reference PMT output charge at the reference voltage, V_{ref} and n is the number of PMT dynodes. In the present case, n=8. We take as reference output charge at V_{ref}=-400 V and plot the response between -400 and -1000 V. The model is generated for both prototype fibers and shows excellent agreement with the data over the voltage range.

Operations

We began exploration of the PAR fast loss monitor by mounting a 4-m length of FO cable on the outboard side of the beam chamber in the SW octant as shown in Fig 3a.

06 Beam Instrumentation, Controls, Feedback, and Operational Aspects

T18 Radiation Monitoring and Safety

An example of successive loss signals observed from the chamber-mounted fiber during injection is presented in Figure 6. We found that intraturn loss patterns were resolvable
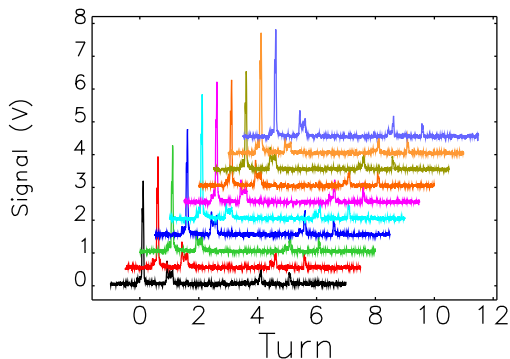

Figure 6: Successive injection losses observed with the chamber-mounted fiber.

and varied from shot-to-shot. Since peak loss signals from the chamber were often saturated, and since a more pressing need was to determine the losses occurring at the shield walls, a second prototype fiber bundle of identical design was installed on the south shield wall as shown in Fig. 3b.

Beam Loss Studies

Several dedicated loss studies were conducted with the prototype FO cable, including two with the cable mounted to the shield wall in various locations giving sensitivity to different loss scenarios. The variation of fast BLM output current (PMT output charge per acceleration period) with a signal from a radiatio monitor (LP6) outside the shield wall is plotted in Figure 7, as injected charge is varied from 1 to 4 nC. Also presented in the figure are the fast BLM pulses for the case of 4 nC. Each linac pulse injects 1 nC of charge
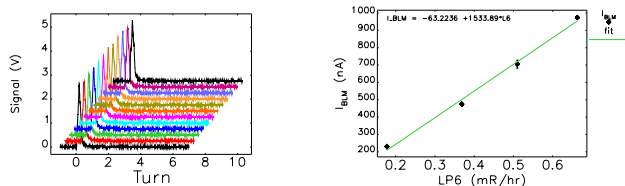
(a) BLM waveforms for 4 nC.   (b) Fast BLM current with LP6.

Figure 7: Loss study calibration of fast BLM prototype.

into the PAR, so the shape of the loss pulse stays roughly the same from shot to shot.

INTERLOCK SYSTEM

A concept for an interlock based on FO detectors has been explored, in which an analog circuit will integrate the PMT output pulses over a given time period, and trigger a safety trip if the integrator output exceeds a predetermined limit [13]. In the simplest implementation, the integrator would run

continously and decay with a time constant that would be matched to the loss profile.

The addition of an FPGA and ADC are also being investigated. The FPGA will control the analog integrator and ADC based on external timing signals, and will also provide digital processing of the data in order to generate safety trips. The external timing signals will allow processing based on the linac beam rates (1-30Hz) and PAR-Booster rates (1 or 2 Hz), depending on the machine conditions. Block diagrams of the analog and digital (FPGA) versions of the interlock circuit are shown in Figure 8.
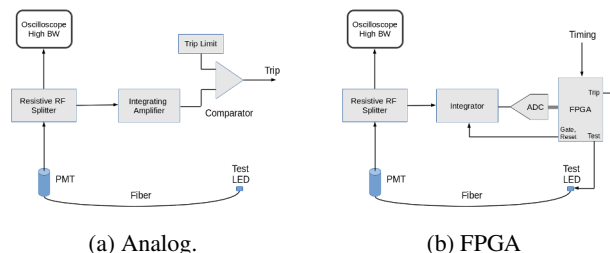
(a) Analog.   (b) FPGA

Figure 8: Interlock circuit block diagrams.

DISCUSSION AND SUMMARY

We have demonstrated the feasibility of an FO-based interlock system, but a considerable effort remains to turn it into an accredited system. Hence, the present plan is to develop the fast BLM system as a diagnostic and move forward with enhanced shielding. The fast FO BLM can clearly see beam loss at relevant levels for personnel protection, and is sufficiently radiation resistant and reliable to be operated for extended periods of time. The fast BLM diagnostic would be implemented with a 20-m length FO cable, similar in cross section to the prototype, covering the south, southeast, and east PAR shield walls, providing contiguous monitoring along this portion of the wall. A fast FO-based BLM interlock system can be made intelligent; for example, the system is fast enough to see turn-by-turn (TBT) patterns (t_{rise}=2-3 ns) which may indicate when losses are about to become excessive. We are presently discussing the details of the enhanced shielding. In principle, with sufficient lead we can mitigate the radiological risk from any beam loss scenario; however, such solution is not without cost and may impose access restrictions around the PAR.

ACKNOWLEDGMENTS

Thanks to C. Clarke, A. Fisher, and others involved in the LCLS-II BCS effort at SLAC for useful and helpful interactions. Thanks also to P. Dombrowski for his assistance with hardware installation.

REFERENCES

[1] C. Clarke et al. "LCLS-II Beam Containment System for Radiation Safety," in Proc. FLS2018, Shanghai, China, March 2018, paper THP1WD02, in process.

[2] T. Obina , Y. Yano, "Optical Fiber Based Loss Monitor for Electron Storage Ring," in Proc. IBIC2013, Oxford, UK, 2013, paper WECL1, pp. 638-643.

[3] A. Kaukher, I. Krouptchenkov, D. Noelle, H. Tiessen, K. Wittenburg, "XFEL Beam Loss Monitor System," in Proc. BIW2012, Newport News, VA USA, paper MOPG007, pp. 35-37.

[4] J. Dooling, K. Harkay, V. Sajaev, and H. Shang, "Operational Experience with Fast Fiber-Optic Beam Loss Monitors for the Advanced Photon Source Storage Ring Superconducting Undulators," Proc. of NAPAC2016, Chicago, IL, USA, 2016, 28-31.

[5] M. Borland et al., "Commissioning of the Argonne Positron Accumulator Ring," PAC 1995, 287 (1996).

[6] M. Borland et al., "The Upgrade of the Advanced Photon Source," these proceedings.

[7] MCNP Code Team, MCNP User's Manual, Code Version 6.2, LA-UR-17-29981 (Oct. 2017).

[8] J. Vacca, private communication, April 23, 2018.

[9] M. Borland, private communication, April 16, 2014.

[10] 10 CFR 835, Occupational Radiation Protection, 1-1-17 edition. https://www.gpo.gov/fdsys/pkg/CFR-2017-title10-vol4/pdf/CFR-2017-title10-vol4-part835.pdf

[11] I. Dumanoglu et al. Nuclear Instruments and Methods in Physics Research A **490** (2002) 444–455.

[12] K. Cankocak et al. "Radiation-hardness measurements of high OH$^-$ – content quartz fibres irradiated with 24 GeV protons up to 1.25 Grad," Nuclear Instruments and Methods in Physics Research A **585** (2008) 20–27.

[13] A. Fisher et al. "Beam Containment And Machine Protection for LCLS-2" Proc. of IBIC17, in process.